Research Article

Antiliver Fibrosis Screening of Active Ingredients from *Apium graveolens* L. Seeds via GC-TOF-MS and UHPLC-MS/MS

Ming Qiao [ID],[1] **Jianhua Yang,**[2] **Yao Zhao,**[1] **Yi Zhu,**[2] **Xiaomei Wang** [ID],[1] **Xinling Wang,**[1] **and Junping Hu** [ID][1]

[1]*College of Pharmacy, Xinjiang Medical University, Urumqi 830011, China*
[2]*Department of Pharmacy, The First Affiliated Hospital, Xinjiang Medical University, Urumqi 830011, China*

Correspondence should be addressed to Junping Hu; hjp-yft@163.com

Although several studies have been performed on *Apium graveolens* L.(celery) seeds, their antiliver fibrosis effects remain to be unexplored. Firstly, we detected the effects of celery seeds extracted with different concentrations of aqueous ethanol on the proliferation of HSC-LX2 cells. Then, we detected the effects of fractions of the optimal effect extract on the proliferation and apoptosis of HSC-LX2 cells. Finally, the compounds of petroleum ether (PP), ethyl acetate (PE), n-butyl alcohol (PB), and water fractions (PW) of the optimal effect extract were determined by GC-TOF-MS and UHPLC-MS/MS, to confirm the potentially antifibrotic compounds combined with pharmacodynamic experiment of monomer compounds *in vitro*. The results revealed that 60% ethanol extract of celery seeds (60-extract) exhibited remarkable inhibition effect on the proliferation of HSC-LX2 cells compared with 95% ethanol and aqueous extract. Besides, it validated that the inhibition rates of PP, PE, PB, and PW on the proliferation of HSC-LX2 cells were 75.14%, 73.52%, 54.09%, and 43.36%, and their percentage of apoptotic cells were 37.5%, 4.3%, 0.7%, and 0.1% at high doses, respectively. Additionally, it was manifested that apigenin, aesculetin, and butylphthalide have major contribution to the overall compounds of celery seeds, and the inhibition effects on the cell proliferation clearly elevated with increase in their contents. In essence, apigenin, aesculetin, and butylphthalide may hopefully become the natural products of antiliver fibrosis, which laid a foundation for the subsequent development of celery seeds as antiliver fibrosis drugs.

1. Introduction

Liver fibrosis is the essential pathophysiologic consequence of chronic hepatic injury [1]. Without favorable treatment, liver fibrosis can develop into cirrhosis, which is estimated to affect 1% to 2% of global population and result in over 1 million deaths annually worldwide [2, 3]. The major causes of liver fibrosis include chronic hepatitis virus infection, alcohol abuse, and nonalcoholic steatohepatitis [4]. Hepatic fibrosis is characterized by excessive accumulation of extracellular matrix (ECM) caused by both increased synthesis and deposition of newly formed components and decreased or unbalanced degradation of ECM [5]. Hepatic stellate cell (HSC) activation is considered as a pivotal event in liver fibrosis, which is mainly responsible for the excessive accumulation of ECM proteins in the liver [6, 7]. Nowadays, a growing body of basic and clinical evidences have

manifested that liver fibrosis can be reversed after the cessation of injurious stimulus [8, 9]. Hence, the development of antiliver fibrosis drugs is an urgent demand at present.

Apium graveolens L.(celery) belongs to the family Apiaceae, which is grown as a vegetable in many parts of the world [10]. It is rich in compounds including limonene, selinene, glycosides, flavonoids, and vitamins [11]. These constituents are also reported to prevent cardiovascular diseases [12], jaundice [13], urinary tract obstruction [14], gout [15], and rheumatic disorders [16, 17]. Celery seeds are spicy, carminative [18], diuretic [19], appetizer [20], stimulant, hypotensive [21], aphrodisiac, anti-inflammatory, and laxative [22]. In addition, celery seeds are also widely used in Chinese compound preparations to protect the liver, such as Huganbuzure Granule, Ganbaokang Granule, Fufangzupa Syrup, and Mawuliwusuli Granule [23, 24]. However, there is no report for pharmacological activity of celery seeds on

the antiliver fibrosis. Therefore, transforming growth factor-$\beta1$ (TGF-$\beta1$) induced HSC-LX2 cells to establish a liver fibrosis model *in vitro* to investigate the antiliver fibrosis effect of active fractions and compounds of celery seeds combined with GC-TOF-MS and UHPLC-MS/MS techniques.

2. Materials and Methods

2.1. Materials. *Apium graveolens* L. seeds were purchased from the decoction factory of Xinjiang Madison Medicine (Xinjiang, China). The botanical identification of the plant material was performed by Dr. Jianhua Yang from the first affiliated hospital of Xinjiang Medical University. The voucher specimen was deposited at the department of pharmacognosy of Xinjiang Medical University. Methanol, acetonitrile, and formic acid (HPLC grade) were obtained from Merck (Darmstadt, Germany). L-2-chlorophenylalanine and BSTFA (HPLC grade) were supplied by Sigma (St. Louis, MO, USA). Ultrapure water was prepared with a Milli-Q system (Millipore, Milford, MA, USA). Ethyl alcohol, petroleum ether, ethyl acetate, and n-butyl alcohol were of analytical grade.

2.1.1. Preparation of the Extracts. The celery seed extracts were prepared according to the reflux extraction, by adding 8 times the amount of distilled water, 60% and 95% aqueous ethanol (v/v) to 50.00 g of the dried celery seeds, respectively, and heating reflux 3 times (3×1.5 h) at 60°C. The filtrates were combined and concentrated with a rotary evaporator (IKA, Staufen, Germany) to obtain aqueous extract, 60% and 95% ethanol extracts, and the yields were 8.6%, 3.8% and 12.8%, respectively.

2.1.2. Preparation of the Fractions and Monomeric Compounds from Celery Seeds. Celery seeds (8.00 kg) were refluxed thrice with 8 times the amount of 60% ethanol at 60°C, and the extracts were combined and evaporated under reduced pressure to afford 200.6 g of crude extract. The 60% ethanol extract was dissolved in water to produce an aqueous solution, and then partitioned in turn with petroleum ether, ethyl acetate, and n-butyl alcohol to afford petroleum ether (PP, 5.12 g), ethyl acetate (PE, 20.80 g), n-butyl alcohol (PB, 70.60 g), and water-soluble (PW, 89.60 g) fractions after drying. Nine compounds were isolated from PP, PE, PB, and PW. Their structures were identified as apigenin (8.3 mg) [25], 5-methoxypsoralen (10.2 mg) [26], apiin (9.1 mg) [27], rutin (7.7 mg) [28], kaempferol (9.3 mg) [29], luteolin (6.1 mg) [30], quercetin (6.2 mg) [31], mollugin (5.6 mg) [32], and butylphthalide (8.0 mg) [33] by using extensive spectroscopic analysis including ^{1}H-NMR and ^{13}C-NMR.

2.1.3. Samples for GC-TOF-MS and UHPLC-MS/MS Analysis. 100 μL of PP was extracted with methanol and added 10 μL of L-2-chlorophenylalanine as internal standard and vortex (Grant, Cambridge, UK) mixed for 30 seconds. Then it was centrifuged at 4°C for 15 min at 12000 rpm using

a centrifuge (Thermo Fisher, Waltham, USA). 100 μL of supernatant was transfered and dried completely in a vacuum concentrator (Retsch, Arzberg, Germany). To add 60 μL of the BSTFA reagent to the sample aliquots, it is incubated for 1.5 hours at 70°C. The sample was analysed by GC-TOF-MS. The PE, PB, and PW were thawed on the ice. Then the samples were centrifuged at 12000 rpm for 15 min at 4°C, and 200 μL of supernatant of the sample was dried under a gentle nitrogen flow. The residue was reconstituted with 200 μL of methanol. Then the samples were centrifuged at 12000 rpm for 10 minutes at 4°C. The resulting supernatants were transferred to 2 mL of sample vials and stored at −80°C until the UHPLC-MS/MS analysis.

2.2. Cell Culture. HSC-LX2 cells (Applied Biosystems, Foster City, USA) were cultured in a high-glucose Dulbecco's modifed eagle medium (HG-DMEM, Gibco, Grand Island, USA) supplemented with 10% FBS (Gibco, Grand Island, USA), 100 μg·mL^{-1} streptomycin, and 100 U·mL^{-1} penicillin (Gibco, Grand Island, USA). The cells were maintained in a humidified incubator with 5% CO$_2$ at 37°C, and they were subcultured every 2 days to maintain logarithmic growth.

2.3. Establishment of the Liver Fibrosis Model Induced by TGF-$\beta1$. The logarithmic phase cells were inoculated in a 96-well plate at a density of 2×10^3 cells per well and treated with TGF-$\beta1$ (Novoprotein, Shanghai, China) at concentrations of 5, 10, 20, 40, 80, and 100 ng·mL^{-1} for 24, 48, and 72 h. Blank group (containing all reagents except the studied sample) was set. The cell viability was assessed by cell-counting kit-8 (CCK-8) assay (Solarbio, Beijing, China). The absorbance was determined at 450 nm using multiscan spectrum (Multiskan GO, Thermo Fisher, Waltham, USA). The hyaluronic acid (HA), laminin (LN), and type III procollagen (PCIII) levels were determined using enzyme-linked immunosorbent assay (ELISA) kits (Jianglai Biological, Shanghai, China). All conditions were performed in triplicate, and each experiment repeated for three times. Cell viability was calculated as follows:

$$\text{Cell viability} (\%) = \left[\frac{\left(\text{OD}_{450\,(\text{TGF}-\beta1)} - \text{OD}_{450\,(\text{solvent})} \right)}{\left(\text{OD}_{450\,(\text{blank})} - \text{OD}_{450\,(\text{solvent})} \right)} \right] \times 100. \tag{1}$$

2.4. Cell Proliferation Assay. HSC-LX2 cells were plated on 96-well plates at a density of 5×10^3 cells per well and treated with various concentrations of extracts and fractions of celery seed in combination with 100 ng·mL^{-1} of TGF-$\beta1$ for 48 h. Blank group (containing all reagents except the studied sample) was set. The positive control group was added with 50 μg·mL^{-1} of the compound Biejiaruangan Troche (BJRG) (Inner Mongolia Furui Medical Science, Inner Mongolia, China). 100 ng·mL^{-1} of TGF-$\beta1$ was added to the model group. The absorbance was quantified at 450 nm using a multiscan spectrum. Additionally, the HA, LN, and PCIII

levels were also performed by ELISA kits. Each treatment was performed in triplicate, and each experiment was

repeated for three times. Cell inhibiting rate was calculated as follows:

$$\text{cell inhibiting rate (\%)} = \left[1 - \left[\frac{\left(\text{OD}_{450\,(\text{sample})} - \text{OD}_{450\,(\text{solvent})}\right)}{\left(\text{OD}_{450\,(\text{TGF}-\beta 1)} - \text{OD}_{450\,(\text{solvent})}\right)}\right]\right] \times 100. \tag{2}$$

2.5. Cell Apoptosis. Annexin V-FITC Apoptosis Detection Kit (Becton Dickinson, Franklin Lakes, NJ, USA) was utilized for cell apoptosis analysis according to the manufacturer's instruction. Cells were divided into viable cells, dead cells, early apoptotic cells and apoptotic cells, and analyses were performed on the flow cytometer (Becton Dickinson, Franklin Lakes, NJ, USA). The ratio of apoptotic cell reflected the proapoptotic effect of PP, PE, PB, and PW of 60% ethanol extract from celery seeds. Each treatment was repeated in triplicate.

2.6. GC-TOF-MS Analysis. The Agilent 7890 gas chromatograph system is coupled with a Pegasus HT time-of-flight mass spectrometer. The system utilized a DB-5MS capillary column coated with 5% diphenyl cross-linked with 95% dimethylpolysiloxane (30 m × 250 μm, 0.25 μm; J&W Scientific, Folsom, CA, USA). An aliquot of the analyte (1 μL) was injected into the GC/MS apparatus. Helium was the carrier gas at a flow rate of 1 mL·min^{-1}. GC oven temperature started at 50°C and was held for 1 min at 310°C and then for 10 min with program rate 10°C·min^{-1}. The injector and detector temperatures were set at 280°C and 250°C, respectively. The mass spectrometer was run in the electron ionization mode (−70 eV).

2.7. UHPLC-MS/MS Analysis. Chromatographic analysis was performed in an Agilent 1290 ultra-high performance liquid chromatography (Agilent, Technologies, CA, USA). An ACQUITY ULC HSS T3 column (2.1 mm × 100 mm, 1.8 μm, Waters, USA) was used for separation with gradient elution of 0.1% formic acid aqueous solution (A) and acetonitrile (B), and the column temperature was maintained at 40°C. The detailed gradient conditions were 0–2 minutes, 0%–2% B; 2–11 minutes, 2%–98% B; and 11–13 minutes, 98%–2% B. The flow rate was 0.3 mL·min^{-1}, and the injection volume was 10 μL. Mass spectrometry was performed on the AB Sciex QTrap 6500 (AB SCIEX, Los Angeles, CA, USA) for characterization equipped with electrospray ionization (ESI) source in both positive and negative ionization multiple reaction monitoring (MRM) mode. The parameters were set as follows: nebulizer gas of 60 psi; heater gas of 55 psi; curtain gas of 35 psi; ionspray voltage of +5500/−4500 V; ion transfer tube temperature of 550°C.

2.8. Screening of Antiliver Fibrosis Activity of Monomeric Compounds. Briefly, cells were seeded onto a 96-well plate at a density of 5×10^3 cells per well. Cells were exposed to different concentrations of compounds with 100 ng·mL^{-1} TGF-β1 24 h after seeding. The positive control group was

added with 50 μg·mL^{-1} of BJRG. Each treatment was repeated in triplicate. After 48 h of sample incubation at 37°C, CCK-8 solution was added to each well. After a further 1 h of incubation, the absorbance of each well was measured at 450 nm, and cell inhibiting rate was calculated.

2.9. Statistical Analysis. The results of cell experiment were expressed as the mean standard deviation of three parallel measurements, and statistical significance was assessed using one-way analysis of variance (ANOVA) followed by a multiple comparison test (Tukey's post-hoc test), where $P < 0.05$ and $P < 0.01$ were considered significant. Three injections used in the GC-TOF-MS and UHPLC-MS/MS analysis, and the relative percentage of the compound was the average of the normalized values of the three determinations of the peak area.

3. Results

3.1. Effects of TGF-β1 on the Proliferation of HSC-LX2 Cells. We used six concentrations and three time points of TGF-β1 to explore the proliferation of HSC-LX2 cells (Table 1). At given time points, HSC-LX2 cells viability clearly elevated with increased TGF-β1 concentrations. The HSC-LX2 cells viability remarkably decreased with prolonged time. Absorbance peaked at 48 h with 100 ng·mL^{-1} of TGF-β1 and abated gradually later. Therefore, HSC-LX2 cells were activated by 100 ng·mL^{-1} of TGF-β1 for 48 h to establish a liver fibrosis model.

3.2. Effects of TGF-β1 on Liver Fibrosis Indexes. As expected, serum HA, LN, and PCIII levels were remarkably elevated after TGF-β1 treatment in comparison with the blank control group. It indicated that the liver fibrosis model was established successfully *in vitro* (Table 2).

3.3. Effects of Extracts and the Fractions of Celery Seeds on Proliferation of HSC-LX2 Cells. HSC-LX2 cells were notably activated by TGF-β1, as shown in Table 3. The results indicated that celery seed extracts and its fractions inhibited HSC-LX2 cell proliferation in a dose-dependent fashion. 60% ethanol extract showed a stronger inhibitory effect than the aqueous extract and 95% ethanol extract. The inhibition rates of PP, PE, PB, and PW were 75.14%, 73.52%, 54.09%, and 43.36% at high doses, respectively.

3.4. Effects of PP, PE, PB, and PW on Liver Fibrosis Indexes. TGF-β1 treatment caused a remarkable collagen accumulation. In sharp contrast, treatment with PW, PB, PE, and PP

TABLE 1: Effects of TGF-β1 on the viability of HSC-LX2 cells (mean ± SD, $n = 3$).

Group	Dose (ng·mL^{-1})	24 h OD	24 h Viability (%)	48 h OD	48 h Viability (%)	72 h OD	72 h Viability (%)
Solvent control	—	0.183 ± 0.004	—	0.175 ± 0.004	—	0.210 ± 0.001	—
Blank control	—	0.395 ± 0.102	—	0.671 ± 0.023	—	1.739 ± 0.197	—
TGF-β1	5	0.347 ± 0.054	77.35 ± 0.75	0.711 ± 0.072	108.11 ± 3.26	0.573 ± 0.109$^{\#}$	23.76 ± 2.65
	10	0.501 ± 0.028	150.72 ± 0.62	0.775 ± 0.042	121.10 ± 2.61	0.596 ± 0.035$^{\#}$	25.24 ± 2.41
	20	0.511 ± 0.067	154.71 ± 0.86	0.820 ± 0.103	130.12 ± 4.51	1.316 ± 0.136	47.63 ± 1.04
	40	0.695 ± 0.105$^{\#}$	215.52 ± 1.96	0.894 ± 0.110	145.21 ± 5.62	1.311 ± 0.185	72.13 ± 3.65
	80	0.640 ± 0.108$^{\#}$	241.49 ± 0.21	1.093 ± 0.079$^{\#}$	177.59 ± 2.54	2.472 ± 0.145$^{\#}$	148.51 ± 2.54
	100	0.803 ± 0.101$^{\#}$	292.45 ± 0.26	1.755 ± 0.081$^{\#\#}$	318.39 ± 6.26	2.728 ± 0.177$^{\#}$	164.54 ± 3.22

Compared with the blank control group ($^{\#}P < 0.05$, $^{\#\#}P < 0.01$).

TABLE 2: Effects of TGF-β1 on liver fibrosis indexes (mean ± SD, $n = 3$).

Group	Dose (ng·mL^{-1})	LN (μg·L^{-1})	HA (ng·L^{-1})	PCIII (μg·L^{-1})
Blank control	—	51.8 ± 0.78	26.9 ± 5.67	18.8 ± 4.53
Model group (TGF-β1)	100	833.4 ± 9.94$^{\#\#}$	302.3 ± 7.44$^{\#\#}$	115.3 ± 3.38$^{\#\#}$

Compared with the blank control group ($^{\#}P < 0.05$, $^{\#\#}P < 0.01$).

TABLE 3: Effects of the extracts and fractions of celery seeds on inhibition of HSC-LX2 cell proliferation (mean ± SD, $n = 3$).

Group	Fraction	Dose (μg·mL^{-1})	OD	Inhibition ratio (%)
Solvent control		—	0.254 ± 0.019	—
Blank control		0	1.021 ± 0.079	—
Model group (TGF-β1)		0.1	3.522 ± 0.178$^{\#\#}$	—
BJRG		50	1.116 ± 0.012**	73.11 ± 0.87
Aqueous extract of celery seeds		50	3.532 ± 0.227$^{\#\#}$	—
		100	3.074 ± 0.131$^{*\#\#}$	13.79 ± 2.91
		200	2.537 ± 0.541$^{*\#}$	30.13 ± 1.02
95% ethanol extract of celery seeds		50	3.602 ± 0.281	—
		100	2.926 ± 0.0526$^{*\#}$	18.22 ± 1.69
		200	1.717 ± 0.026$^{**\#}$	55.22 ± 2.44
60% ethanol extract of celery seeds		50	2.123 ± 0.138$^{**\#}$	42.75 ± 2.21
		100	1.351 ± 0.052**	66.42 ± 1.53
		200	1.097 ± 0.022**	74.20 ± 2.38
	PP	25	2.598 ± 0.224$^{*\#}$	28.26 ± 1.29
		50	1.619 ± 0.129$^{**\#}$	58.21 ± 2.11
		75	1.066 ± 0.023**	75.14 ± 1.45
	PE	25	2.893 ± 0.159$^{*\#}$	19.23 ± 1.32
		50	2.001 ± 0.239$^{**\#}$	46.55 ± 3.87
		75	1.119 ± 0.312**	73.52 ± 2.36
	PB	25	2.956 ± 0.239$^{*\#}$	17.30 ± 3.13
		50	1.916 ± 0.209$^{**\#}$	49.24 ± 2.03
		75	1.754 ± 0.241$^{**\#}$	54.09 ± 1.44
	PW	25	3.369 ± 0.319$^{\#\#}$	4.68 ± 0.75
		50	2.889 ± 0.162$^{*\#}$	19.36 ± 1.72
		75	2.105 ± 0.311$^{**\#}$	43.36 ± 3.55

Compared with the blank control group ($^{\#}P < 0.05$, $^{\#\#}P < 0.01$); compared with the model group ($^{*}P < 0.05$, $^{**}P < 0.01$).

markedly decreased hepatic collagen matrix accumulation, as shown in Table 4. The serum LN, HA, and PCIII contents were markedly reduced in the PE and PP groups, and that of PP groups were closer to the control groups. PW, PB, PE, and PP exhibited different degree in antiliver fibrosis, which might be related to the active component contents.

3.5. Apoptosis Analysis. Annexin V-FITC/PI double staining and flow cytometry were performed to compare the apoptotic rates of HSC-LX2 cells in different groups. As shown in Figure 1, the percentage of apoptotic cells was 0.1% in the control group (Figure 1(a)), that of the group treated with BJRG, PP, PE, PB, and PW were 2.6%, 37.5%, 4.3%, 0.7%,

TABLE 4: Effects of PP, PE, PB, and PW on liver fibrosis indexes (mean $\pm$ SD, $n = 3$).

Group	Dose ($\mu g \cdot mL^{-1}$)	LN ($\mu g \cdot L^{-1}$)	HA ($ng \cdot L^{-1}$)	PCIII ($\mu g \cdot L^{-1}$)
Blank control	0	51.8 ± 0.78	26.9 ± 5.67	18.8 ± 4.53
BJRG	50	$211.0 \pm 5.08^{**}$	$64.5 \pm 3.19^{*}$	$29.2 \pm 2.53^{**}$
Model group (TGF-β1)	0.1	$833.4 \pm 9.94^{\#\#}$	$302.3 \pm 7.44^{\#\#}$	$115.3 \pm 3.38^{\#\#}$
PW	75	$638.27 \pm 7.22^{\#\Delta\Delta}$	$178.82 \pm 3.94^{\#*\Delta}$	$108.87 \pm 9.29^{\#\#\Delta\Delta}$
PB	75	$502.56 \pm 5.85^{\#*\Delta\Delta}$	$111.37 \pm 4.95^{\#*\Delta}$	$78.36 \pm 5.22^{\#\Delta}$
PE	75	$118.40 \pm 5.74^{**}$	$70.80 \pm 7.07^{*}$	$28.30 \pm 0.21^{**}$
PP	75	$97.32 \pm 6.30^{**}$	$30.91 \pm 5.22^{**}$	$19.01 \pm 4.26^{**}$

Compared with the blank control group ($^{\#}P < 0.05$, $^{\#\#}P < 0.01$); compared with the model group ($^{*}P < 0.05$, $^{**}P < 0.01$); compared with the PP group, ($^{\Delta}P < 0.05$, $^{\Delta\Delta}P < 0.01$).
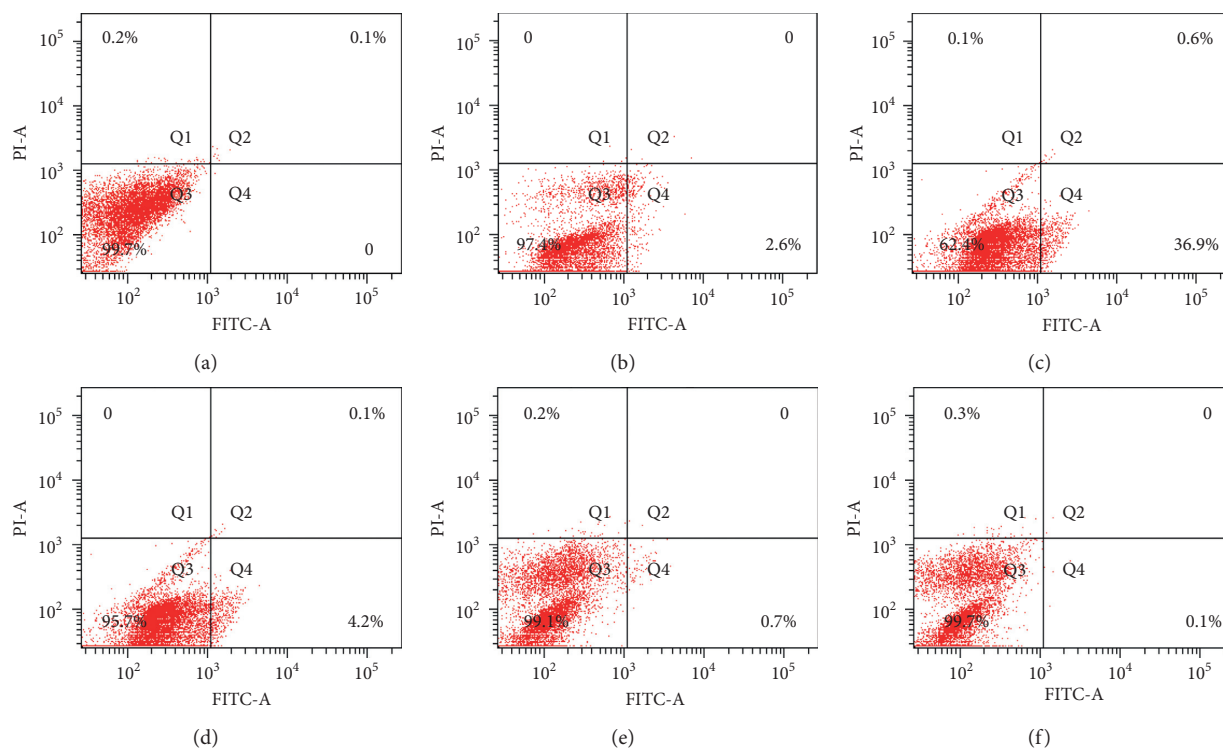
FIGURE 1: Effects of PP, PE, PB, and PW on apoptosis of HSC-LX2 cells. (a) Control. (b) BJRG. (c) PP. (d) PE. (e) PB. (f) PW.

and 0.1%, respectively (Figures 1(b)–1(f)). PP showed stronger proapoptotic function than that of the positive control.

3.6. Analysis of the Fractions of Celery Seeds Using GC-TOF-MS and UHPLC-MS/MS Methods. Identification of several compounds was enabled by comparison of retention times, MS spectra, and MS/MS spectral data with the standard substance and reference materials reported in the literature. According to our knowledge, the chemical compositions of the fractions from celery seeds, investigated by GC-TOF-MS and UHPLC-MS/MS, was performed for the first time in this study. 122 chemical components were identified from PP, PE, PB, and PW through analysis of GC-TOF-MS and UHPLC-MS/MS (Table 5). The obtained total ion chromatograms are shown in Figure 2. The 378 peaks of PP were separated in GC and preliminarily identified 39 main compounds belonging to different chemical families by

TOF-MS which account for 94.32% of total peak area. Chemical composition analysis showed that phenyl peptides accounted for 24.56% acids, 22.96% aldehydes 19.37%, flavonoids 18.42%, alcohols 3.24%, and major compounds were farnesal 19.37%, butylphthalide 18.42%, 4-hydroxymethyl 3-methoxyphenoxyacetic acid 13.54%, aesculetin 13.28%, and apigenin 11.28%.

Of all the compounds detected by UHPLC-MS/MS, 90 compounds were identified by searching the Biotree DB Database and comparing their retention times and MS spectra with the reference literature. 52 chemical constituents were identified from PE, mainly flavonoids, amides, pigments, and ketones, accounting for 75.86% of the total peak area. The major constituents that have been determined through UHPLC-MS/MS analyses were apigenin 8.48%, 2-acetyl-1-ethylpyrrole 5.22%, aesculetin 4.32%, and 2-phenylacetamide 3.86%. 48 compounds were identified from PB, mainly glycosides, esters, aldehydes, and ketones, accounting for 81.88% of the total peak area. The main

TABLE 5: Identification of chemical compositions of fractions from celery seeds.

No.	RT[a] (min)	Compound	Peak Area[b] (%)			
			PW	PB	PE	PP
1	0.69	6-Hydroxyangelicin	0.40	—	—	—
2	0.89	Mannitol	—	0.43	—	—
3	0.91	3-Buten-2-one 1-(2,3,6-trimethyl phenyl)	1.37	0.23	—	—
4	0.96	Lactulose	—	0.28	—	—
5	0.97	Ectoine	—	1.81	—	—
6	0.98	Heptyl formate	0.45	0.38	—	—
7	0.99	Genipic acid	0.45	—	—	—
8	1.00	2,4-Diethylthiazole	—	1.56	—	—
9	1.05	2,5-Dioxopentanoate	2.18	—	—	—
10	1.24	2-Hydroxyethanesulfonate	0.40	0.39	—	—
11	1.27	2,6-Piperidinedicarboxylic acid	1.09	—	—	—
12	1.37	Pregabalin	1.99	—	—	—
13	1.38	N-acetylhistamine	1.46	—	—	—
14	1.38	Nipecotic acid	11.99	1.51	—	—
15	1.39	4-Guanidinobutanoic acid	—	0.25	—	—
16	1.44	Gln gly	1.87	—	—	—
17	1.52	Cytarabine	—	0.74	—	—
18	1.62	Ser val gly	—	2.46	—	—
19	1.74	Ormetoprim	0.29	—	—	—
20	2.02	6-Hydroxynicotinic acid	—	—	0.33	—
21	2.54	3,3,5-Triiodo-L-thyronine-beta-D-glucuronoside	—	0.35	—	—
22	3.13	2-Phenylacetamide	0.63	0.52	3.86	0.10
23	4.1	(S)-5′-deoxy-5′-(methylsulfinyl)adenosine	—	0.54	—	—
24	4.12	Adenine	—	1.88	—	—
25	4.12	Adenosine	0.39	14.99	0.47	—
26	4.19	Cordycepin	—	0.32	—	—
27	4.31	Patulin	0.42	—	—	—
28	4.34	4-Pyridoxic acid	—	0.27	0.36	—
29	4.35	Inosine	—	0.94	—	—
30	4.36	3′-Deoxyadenosine	—	—	0.41	—
31	4.39	α-[1-(ethylamino)ethyl]-p-hydroxy- benzyl alcohol	—	—	0.56	—
32	4.93	Selfotel	1.51	—	—	—
33	4.98	2-Acetyl-1-ethylpyrrole	3.72	0.30	5.22	0.08
34	4.99	3-Aminobenzamide	0.87	—	0.93	—
35	5.01	4-Hydroxydihydrocinnamaldehyde	—	—	0.36	—
36	5.11	Imidazoleacetic acid	—	—	0.79	—
37	5.16	Mequinol	0.34	2.55	—	—
38	5.36	2-Pyrocatechuic acid	0.62	—	0.85	—
39	5.36	L-tryptophan	1.52	0.44	—	—
40	5.39	Imidacloprid-guanidine	0.39	0.27	1.07	—
41	5.50	Dopamine	—	—	0.50	—
42	5.76	Methiocarb-sulfoxide	0.45	—	—	—
43	5.81	3-(4-methoxy-6-oxopyran-2-yl)butanoic acid	0.51	—	—	—
44	6.24	1-naphthylmethanol	—	—	0.89	—
45	6.41	1H-indole-3-carboxaldehyde	2.65	0.32	1.86	0.38
46	6.73	n-Acetylhomoproline	—	0.23	—	—
47	6.77	Methyl 3-methyl-1-butenyl disulfide	0.75	0.28	—	—
48	6.82	Aesculin	—	—	0.66	—
49	6.87	Oleic acid	—	—	0.47	—
50	6.89	Beta-carboline	—	—	0.86	—
51	6.98	3-Carboxypropyl trimethylammonium	0.43	—	0.39	—
52	6.99	Apigenin	—	—	8.48	11.28
53	7.28	trans-O-hydroxybenzylidenepyruvate	0.35	—	—	—
54	7.31	Eugenitol	0.85	0.22	0.84	—
55	7.54	Glycolic acid	—	—	—	0.18
56	7.59	2-Ketobutyric acid	—	—	—	0.12
57	7.61	Indoleacetic acid	0.44	—	0.43	—
58	7.62	4-Methyl-1-phenyl-2-pentanone	1.35	—	—	—
59	7.66	3-Methyl-1-phenyl-3-pentanol	8.05	—	0.72	—

TABLE 5: Continued.

No.	RT[a] (min)	Compound	Peak Area[b] (%)			
			PW	PB	PE	PP
60	7.69	3′-Methoxy-E,E-dienoestrol	0.36	—	0.70	—
61	7.79	2-Butyl-1-octanol	0.38	—	0.52	—
62	7.80	2-Hydroxy-8-methylchromene-2-carboxylate	0.43	—	1.91	—
63	7.84	Diflufenican	—	1.78	0.82	—
64	7.89	3-Methylbenzaldehyde	0.40	—	0.42	—
65	7.98	Luteolin 7-galactoside	6.59	2.42	0.76	—
66	7.99	2-Naphthol	2.30	0.24	0.94	—
67	8.16	Apiin	2.34	3.64	0.78	—
68	8.17	Ambolin	—	6.72	1.49	—
69	8.19	2-Hydroxymuconate semialdehyde	1.29	5.21	1.53	—
70	8.20	Decanoic acid, 3-amino-, (S)-	—	0.66	2.77	—
71	8.21	Indoleacrylic acid	0.54	—	1.82	—
72	8.22	Glycine	—	—	—	0.11
73	8.27	Aesculetin	0.11	0.56	4.32	13.28
74	8.27	Pelargonidin 3-O-glucoside	—	2.08	2.61	—
75	8.32	Peonidin-3-O-beta-galactopyranoside	0.18	1.95	2.97	—
76	8.46	2-Butyl-3-phenyl-2-propen-1-al	0.79	0.35	0.95	—
77	8.61	1,6-Dimethoxypyrene	0.30	—	2.08	—
78	8.65	Foliosidine	0.51	—	1.76	—
79	8.72	Ensulizole	2.23	—	1.53	—
80	8.73	3-Hydroxypropionic acid	—	—	—	2.61
81	8.84	Flavan skeleton	0.40	—	1.82	—
82	8.92	Chalconaringenin	—	4.87	—	—
83	9.01	Peonidin 3-(6″-acetylglucoside)	—	—	1.82	—
84	9.27	Mesylate	7.13	3.03	0.59	—
85	9.33	15-Methylpalmitate (2R,3R)-2-(3,4-dihydroxyphenyl)-3,5-	0.12	7.18	2.26	—
86	9.40	Dihydroxy-7-methoxy-2,3-dihydrochromen-4-one	1.86	1.17	—	—
87	9.70	α-Terpinene	0.45	0.51	0.37	0.47
88	9.80	4-Methyl-N-ethylcathinone	0.54	1.43	0.86	—
89	9.93	Perillyl acetate	0.65	0.26	1.39	—
90	10.27	5,6,7,8-Tetrahydro-2-naphthol	1.12	2.36	1.49	—
91	10.52	Cicaprost	—	0.25	2.47	—
92	13.72	Erucamide	2.27	0.75	0.80	0.09
93	13.91	Oxoproline	—	—	—	0.16
94	14.52	(2R,3S)-2-Hydroxy-3-isopropylbutanedioic acid	—	—	—	0.16
95	15.44	Vanillin	—	—	—	0.39
96	15.51	Lauric acid	—	—	—	0.17
97	15.80	DL-anabasine	—	—	—	1.79
98	15.93	Phthalic acid	—	—	—	0.35
99	16.01	Methyl jasmonate	—	—	—	1.44
100	16.23	D-arabitol	—	—	—	0.58
101	16.24	Ribitol	—	—	—	0.42
102	16.59	N-(2-hydroxyethyl)-iminodiacetic acid	—	—	—	0.10
103	16.68	Farnesal	—	—	—	19.37
104	16.72	S-carboxymethylcysteine	—	—	—	0.17
105	16.87	Gentisic acid	—	—	—	1.81
106	16.97	terephthalic acid	—	—	—	1.10
107	17.07	Farnesol	—	—	—	0.40
108	17.13	N-acetylisatin	—	—	—	0.16
109	17.64	Myristic acid	—	—	—	0.47
110	17.76	Fructose	0.78	—	—	—
111	18.08	Butylphthalide	—	—	—	18.42
112	18.09	Galactose	0.10	—	—	—
113	18.59	Coniferyl alcohol	—	—	—	0.82
114	18.70	1-Hexadecanol	—	—	—	0.12
115	19.45	4-Hydroxymethyl-3-methoxyphenoxyacetic acid	—	—	—	13.54
116	19.62	Palmitic acid	—	—	—	0.64
117	19.94	Myo-inositol	—	—	—	0.08
118	20.61	6-Hydroxy caproic acid dimer	—	—	—	0.35

TABLE 5: Continued.

No.	RT[a] (min)	Compound	Peak Area[b] (%)			
			PW	PB	PE	PP
119	21.17	Linoleic acid	—	—	—	0.78
120	21.40	Stearic acid	—	—	—	0.76
121	28.89	Cholestan-3beta-ol	—	—	—	0.25
122	30.62	Cholestane-3,5,6-triol, (3beta, 5alpha,6beta)-	—	—	—	0.82
		Total	84.35	81.88	75.86	94.32

RT[a]: retention time (min); Peak Area[b]: the average of the percentage of peak area relative to the total peak area ($n = 3$); "—": not detected.
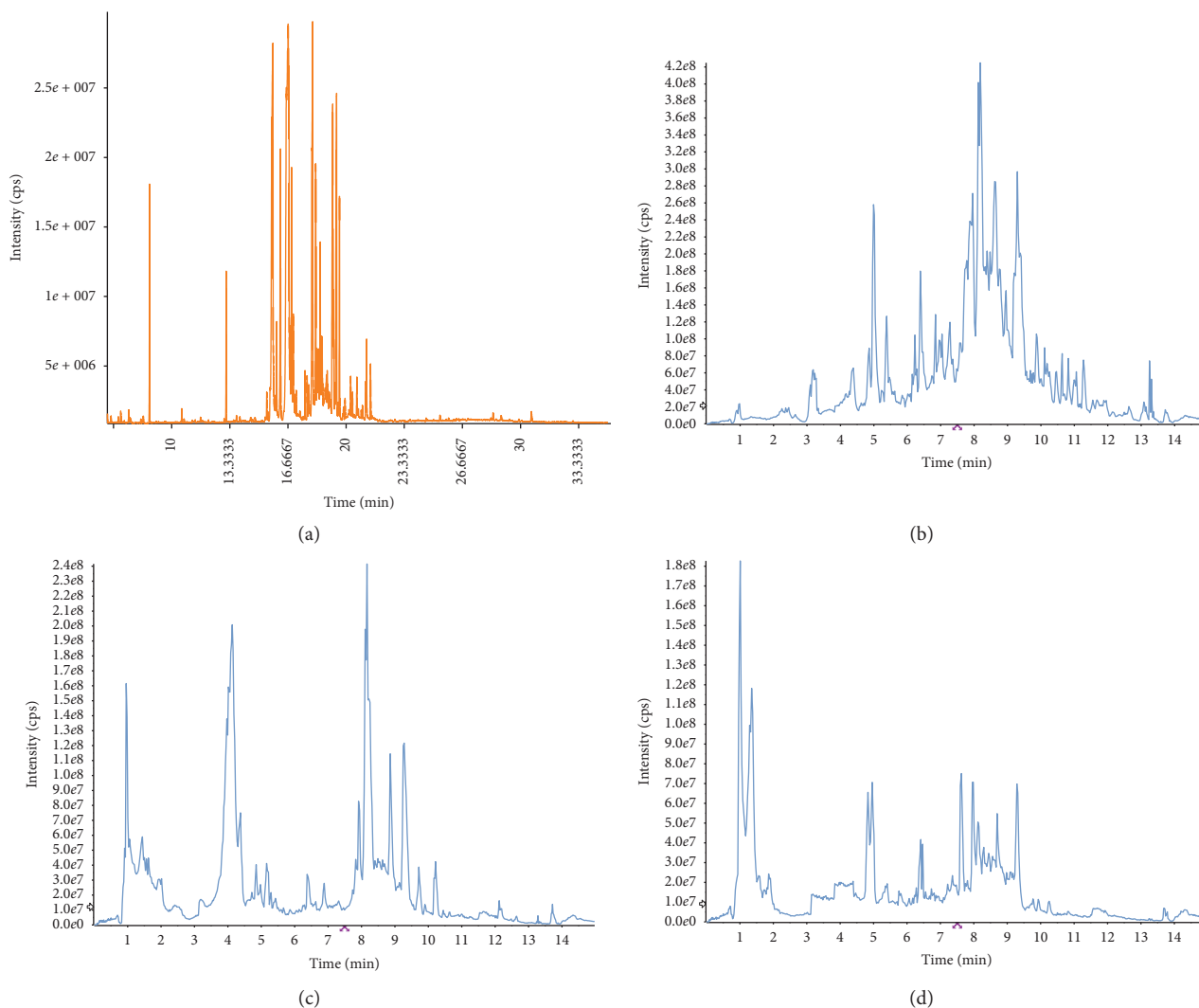
FIGURE 2: Total ion chromatograms of fractions of celery seeds. (a) PP, (b) PE, (c) PB, and (d) PW.

chemical constituents were adenosine 14.99%, 15-methyl-palmitate 7.18%, ambolin 6.72%, 2-hydroxymuconate semialdehyde 5.21%, and chalconaringenin 4.87%. 58 chemical compositions were identified from PW, mainly sugars, glycosides, acids, and salts, accounting for 84.35% of the total peak area. Nipecotic acid 11.99%, 3-methyl 1-phenyl-3-pentanol 8.05%, mesylate 7.13%, and luteolin 7-galactoside 6.59% were the main chemical constituents.

Aesculetin, 2-phenylacetamide, 1H-indole-3-carbox-aldehyde, alpha-terpinene, and erucamide all existed in PP,

PE, PB, and PW, and aesculetin accounted for 13.28%, 4.32%, 0.56%, and 0.11%. PB, and PW had 19 components in common, including 2-phenylacetamide, 2-acetyl-1-ethyl-pyrrole, apiin, 2-hydroxymuconate semialdehyde, and 15-methylpalmitate. Apigenin was found in both PP and PE, accounting for 11.28% and 8.48%. It was suggested that the PW, PB, PE and PP exhibited different degree in antiliver fibrosis, which might be related to the active compounds contents combined with the pharmacodynamic experiments and the analysis of components.

TABLE 6: Effects of monomeric compounds on the proliferation of HSC-LX2 cells (mean $\pm$ SD, $n = 3$).

Group	Dose ($\mu g \cdot mL^{-1}$)	OD	Inhibition ratio (%)
Solvent control	—	0.164 ± 0.012	—
Blank control	0	1.210 ± 0.070	—
Model group(TGF-β1)	0.1	$3.325 \pm 0.138^{\#\#}$	—
BJRG	60	$0.939 \pm 0.104^{**}$	75.46 ± 2.11
Apigenin	15	$2.746 \pm 0.167^{*\#}$	18.33 ± 1.48
	30	$1.816 \pm 0.046^{**\#}$	47.72 ± 1.93
	60	$1.071 \pm 0.107^{**}$	71.32 ± 2.41
5-Methoxypsoralen	15	3.337 ± 0.128	—
	30	3.382 ± 0.130	—
	60	3.454 ± 0.117	—
Apiin	15	$3.238 \pm 0.177^{\#\#}$	2.73 ± 0.06
	30	$2.716 \pm 0.184^{*\#}$	19.26 ± 1.30
	60	$2.349 \pm 0.329^{*\#}$	30.87 ± 1.85
Rutin	15	3.412 ± 0.193	—
	30	$3.201 \pm 0.104^{\#\#}$	3.92 ± 0.57
	60	$2.825 \pm 0.184^{*\#\#}$	15.81 ± 2.68
Kaempferol	15	3.462 ± 0.161	—
	30	$3.186 \pm 0.252^{\#\#}$	4.38 ± 1.02
	60	$2.629 \pm 0.177^{*\#}$	22.02 ± 3.93
Luteolin	15	3.329 ± 0.202	—
	30	3.341 ± 0.175	—
	60	3.420 ± 0.330	—
Quercetin	15	$3.186 \pm 0.268^{\#\#}$	4.39 ± 0.75
	30	$2.337 \pm 0.224^{*\#}$	31.26 ± 2.11
	60	$1.798 \pm 0.218^{**\#}$	48.28 ± 2.74
Mollugin	15	3.348 ± 0.152	—
	30	3.350 ± 0.183	—
	60	3.425 ± 0.159	—
Butylphthalide	15	$3.029 \pm 0.249^{\#\#}$	9.36 ± 1.01
	30	$2.366 \pm 0.048^{*\#}$	30.33 ± 2.77
	60	$1.367 \pm 0.164^{**}$	61.93 ± 3.51
Aesculetin	15	$2.426 \pm 0.245^{*\#}$	28.44 ± 4.01
	30	$1.979 \pm 0.122^{**\#}$	42.55 ± 3.14
	60	$1.277 \pm 0.273^{**}$	64.90 ± 4.21

Compared with the blank control group ($^{\#}P < 0.05$, $^{\#\#}P < 0.01$); compared with the model group ($^{*}P < 0.05$, $^{**}P < 0.01$).

3.7. Potential Antiliver Fibrosis Activity of Monomeric Compounds. All apigenin, aesculetin, butylphthalide, quercetin, apiin, kaempferol, and rutin had inhibition effects on HSC-LX2 cell proliferation, and the inhibition effect enhanced with increased compound concentrations (Table 6). Their inhibition rates of high-dose were 71.32%, 64.90%, 61.93%, 48.28%, 30.87%, 22.02%, and 15.81%, respectively. 5-methoxypsoralen, luteolin, and mollugin did not have inhibition effects on the proliferation of HSC-LX2 cells. The above results confirmed the antiliver fibrosis compositions of celery seeds and clarified that differences of antiliver fibrosis effects among PW, PB, PE, and PP.

4. Discussion

Liver fibrosis is a critical link in the development of cirrhosis or hepatocellular carcinoma, and there is presently no effective treatment for liver fibrosis. Consequently, it is indispensable to develop new drugs to ameliorate liver fibrosis [34]. In the preceding work, it presented that the alcohol extract of celery seeds could alleviate liver fibrosis. The outcomes of the current work were in keeping with those of earlier studies and further revealed that apigenin, aesculetin, and butylphthalide might have major contribution to the overall antiliver fibrosis activity of celery seeds. In short, it implied that celery seeds might possess potential treatment effect in liver fibrosis.

Transforming growth factor-β1 (TGF-β1) was considered a vital role in the process of liver fibrosis, which could affect hepatic stellate cell (HSC) activation and collagen deposition [35–38]. Therefore, TGF-β1 is widely employed to establish a liver fibrosis model *in vitro*. The activated HSCs lead to hepatic fibrogenesis by excessive production of extracellular matrix (ECM) components [39], such as hyaluronic acid (HA), laminin (LN), and type III procollagen (PCIII) [40–42]. Liver fibrosis is associated with major alterations in both quantity and composition of ECM [43]. In advanced stage, fibrotic liver contains three to ten times

hepatitis B patients with liver fibrosis," *Evidence-Based Complementary and Alternative Medicine*, vol. 2019, Article ID 2408126, 13 pages, 2019.

[4] Y. Zhang, J. Liu, Y. Ma et al., "Integration of highthroughput data of microRNA and mRNA expression profiles reveals novel insights into the mechanism of liver fibrosis," *Molecular Medicine Reports*, vol. 19, no. 1, pp. 115–124, 2019.

[5] Y. Zhou, X. Lv, H. Qu et al., "Differential expression of circular RNAs in hepatic tissue in a model of liver fibrosis and functional analysis of their target genes," *Hepatology Research*, vol. 49, no. 3, pp. 324–334, 2019.

[6] D. Yang, "Research progress of receptor targeted hepatic stellate cell in treatment of liver fibrosis," *Zhonghua Gan Zang Bing Za Zhi*, vol. 26, no. 8, pp. 630–632, 2018.

[7] S. Tan, Y. Lu, M. Xu et al., "β-arrestin1 enhances liver fibrosis through autophagy-mediated snail signaling," *The FASEB Journal*, vol. 33, no. 2, pp. 2000–2016, 2019.

[8] Z. Liu, P. Zhu, L. Zhang et al., "Autophagy inhibition attenuates the induction of anti-inflammatory effect of catalpol in liver fibrosis," *Biomedicine & Pharmacotherapy*, vol. 103, no. 16, pp. 1262–1271, 2018.

[9] J.-B. Qiao, Q.-Q. Fan, L. Xing et al., "Vitamin A-decorated biocompatible micelles for chemogene therapy of liver fibrosis," *Journal of Controlled Release*, vol. 283, no. 21, pp. 113–125, 2018.

[10] W. Kooti and N. Daraei, "A review of the antioxidant activity of celery (*Apium graveolens* L)," *Journal of Evidence-Based Complementary & Alternative Medicine*, vol. 22, no. 4, pp. 1029–1034, 2017.

[11] P. Chonpatho, P. Boonruam, W. Sukketsiri, P. Hutamekalin, and M. Sroyraya, "The antioxidant and neurochemical activity of *Apium graveolens* L. and its ameliorative effect on MPTP-induced Parkinson-like symptoms in mice," *BMC Complementary and Alternative Medicine*, vol. 18, no. 1, pp. 169–182, 2018.

[12] N. Choosri, S. Tanasawet, P. Chonpathompikunlert, and W. Sukketsiri, "*Apium graveolens* extract attenuates adjuvant induced arthritis by reducing oxidative stress," *Journal of Food Biochemistry*, vol. 41, no. 1, pp. 12276–12283, 2017.

[13] K. Dolati, H. Rakhshandeh, M. Golestani, F. Forouzanfar, R. Sadeghnia, and H. R. Sadeghnia, "Inhibitory effects of *Apium graveolens* on xanthine oxidase activity and serum uric acid levels in hyperuricemic mice," *Preventive Nutrition and Food Science*, vol. 23, no. 2, pp. 127–133, 2018.

[14] Y. He, Y. Shi, A. Zhang, X. Zhang, J. Sun, and L. Tian, "Lipid-lowering and antioxidative effects of *Apium graveolens* L. root flavonoid extracts," *RSC Advances*, vol. 9, no. 46, pp. 26757–26767, 2019.

[15] D. Chen, L. D. Melton, D. J. Gillivray, T. M. Ryan, and P. J. Harris, "Changes in the orientations of cellulose microfibrils during the development of collenchyma cell walls of celery (*Apium graveolens* L.)," *Planta*, vol. 250, no. 6, pp. 1819–1832, 2019.

[16] P. Li, J. Jia, D. Zhang, J. Xie, X. Xu, and D. Wei, "In vitro and in vivo antioxidant activities of a flavonoid isolated from celery (*Apium graveolens* L.)," *Food and Function*, vol. 5, no. 1, pp. 50–60, 2014.

[17] Z. Uddin, A. A. Shad, and J. Bakht, "In vitro antimicrobial, antioxidant activity and phytochemical screening of *Apium graveolens*," *Pakistan Journal of Pharmaceutical Sciences*, vol. 28, no. 3, pp. 1699–1704, 2015.

[18] D. Iyer and U. K. Patil, "Assessment of antihyperlipidemic and antitumor effect of isolated active phytoconstituents from *Apium graveolens* L. through bioassay-guided procedures," *Journal of Dietary Supplements*, vol. 16, no. 2, pp. 193–206, 2019.

[19] J.-X. Liu, K. Feng, G.-L. Wang, Z.-S. Xu, F. Wang, and A.-S. Xiong, "Elevated CO_2 induces alteration in lignin accumulation in celery (*Apium graveolens* L.)," *Plant Physiology and Biochemistry*, vol. 127, no. 6, pp. 310–319, 2018.

[20] K. Feng, J.-X. Liu, A.-Q. Duan et al., "AgMYB2 transcription factor is involved in the regulation of anthocyanin biosynthesis in purple celery (*Apium graveolens* L.)," *Planta*, vol. 248, no. 5, pp. 1249–1261, 2018.

[21] D. Chen, L. Melton, Z. Zujovic, and P. J. Harris, "Developmental changes in collenchyma cell-wall polysaccharides in celery (*Apium graveolens* L.) petioles," *BMC Plant Biology*, vol. 19, no. 1, pp. 81–103, 2019.

[22] Y. Yusni, H. Zufry, F. Meutia, and K. Sucipto, "The effects of celery leaf (*Apium graveolens* L.) treatment on blood glucose and insulin levels in elderly pre-diabetics," *Saudi Medical Journal*, vol. 39, no. 2, pp. 154–160, 2018.

[23] M.-Y. Li, J.-X. Liu, J.-N. Hao et al., "Genomic identification of AP2/ERF transcription factors and functional characterization of two cold resistance-related AP2/ERF genes in celery (*Apium graveolens* L.)," *Planta*, vol. 250, no. 4, pp. 1265–1280, 2019.

[24] Y. A. Crespo, S. L. Bravo, Y. G. Quintana, A. S. T. Cabrera, A. B. del Sol, and D. M. Guzmán Mayancha, "Evaluation of the synergistic effects of antioxidant activity on mixtures of the essential oil from *Apium graveolens* L., *Thymus vulgaris* L. and *Coriandrum sativum* L. using simplex-lattice design," *Heliyon*, vol. 5, no. 6, pp. 1942–1966, 2019.

[25] H. B. Huang, L. Jiang, and J. Liu, "Study on the chemical constituents of *Glechoma longituba*," *Journal of Chinese Medicinal Materials*, vol. 40, no. 4, pp. 844–847, 2017.

[26] X. Luo, X. J. Wang, and Y. W. Zhao, "Chemical constituents from *Notopterygium incisum*," *Chinese Traditional and Herbal Drugs*, vol. 47, no. 9, pp. 1492–1495, 2016.

[27] Y. P. Lin, Y. L. Zong, and H. He, "Chemical constituents of the aerial parts of *Seseliyunnanense Franch*," *Natural Products Research Development*, vol. 19, no. 836, pp. 798–800, 2007.

[28] X. J. Wang, X. Luo, and J. M. Zhou, "Chemical constituents from rhizomes of *Rhodiola wallichiana* var. *cholaensis* and their protective effects on myocardium," *Chinese Traditional and Herbal Drugs*, vol. 47, no. 16, pp. 2822–2826, 2016.

[29] M. M. Yan, S. J. Xiao, and F. Chen, "Chemical constituents of *Hypericum ascyron* L.," *Natural Products Research Development*, vol. 26, no. 11, pp. 1785–1788, 2014.

[30] G. Ablikim, N. Yadikar, and H. Aisa, "Chemical constituents from the residue of *Lavandula angustifolia* and their biological activities," *Chinese Traditional Patent Medicine*, vol. 41, no. 4, pp. 818–822, 2019.

[31] R. L. Li, P. L. Wu, and C. R. Li, "Study on the chemical constituents of the branches and leaves of *Juniperus formosana*," *West China Journal of Pharmaceutical Sciences*, vol. 34, no. 1, pp. 5–9, 2019.

[32] Z. Wang, S. M. Zhao, and G. Z. Zeng, "Chemical constituents from roots and rhizomes of *Rubia oncotricha* and their cytotoxic activities," *China Journal of Chinese Materia Medica*, vol. 43, no. 22, pp. 4462–4468, 2018.

[33] W. H. Chen, G. Shen, and H. S. Chen, "High purity preparation and identification of three phthlide compounds from *Apium graveolens*," *Journal of Pharmaceutical Practice*, vol. 35, no. 2, pp. 138–140, 2017.

[34] M. M. Salah, A. A. Ashour, T. M. Abdelghany, A.-A. H. Abdel-Aziz, and S. A. Salama, "Pirfenidone alleviates

concanavalin A-induced liver fibrosis in mice," *Life Sciences*, vol. 6, no. 12, pp. 1169–1182, 2019.

[35] D. Huang, T. Lin, S. Wang et al., "The liver fibrosis index is superior to the APRI and FIB-4 for predicting liver fibrosis in chronic hepatitis B patients in China," *BMC Infectious Diseases*, vol. 19, no. 1, pp. 878–891, 2019.

[36] J. Day, P. Patel, J. Parkes, and W. Rosenberg, "Derivation and performance of standardized enhanced liver fibrosis (ELF) test thresholds for the detection and prognosis of liver fibrosis," *The Journal of Applied Laboratory Medicine*, vol. 3, no. 5, pp. 815–826, 2019.

[37] H.-C. Tsay, Q. Yuan, A. Balakrishnan et al., "Hepatocyte-specific suppression of microRNA-221-3p mitigates liver fibrosis," *Journal of Hepatology*, vol. 70, no. 4, pp. 722–734, 2019.

[38] F. Zhang, M. Hao, H. Jin et al., "Canonical hedgehog signalling regulates hepatic stellate cell-mediated angiogenesis in liver fibrosis," *British Journal of Pharmacology*, vol. 174, no. 5, pp. 409–423, 2017.

[39] F. Yu, B. Chen, P. Dong, and J. Zheng, "Hotair epigenetically modulates PTEN expression via MicroRNA-29b: a novel mechanism in regulation of liver fibrosis," *Molecular Therapy*, vol. 25, no. 1, pp. 205–217, 2017.

[40] P. Xiong, J. Zhang, D. Xu et al., "Positive feedback loop of YB-1 interacting with Smad2 promotes liver fibrosis," *Biochemical and Biophysical Research Communications*, vol. 484, no. 4, pp. 753–761, 2017.

[41] T. Higashi, S. L. Friedman, and Y. Hoshida, "Hepatic stellate cells as key target in liver fibrosis," *Advanced Drug Delivery Reviews*, vol. 121, no. 12, pp. 27–42, 2017.

[42] W. Wang, R. Dong, Y. Guo et al., "CircMTO1 inhibits liver fibrosis via regulation of miR-17-5p and Smad7," *Journal of Cellular and Molecular Medicine*, vol. 23, no. 8, pp. 5486–5496, 2019.

[43] F. Alegre, P. Pelegrin, and A. Feldstein, "Inflammasomes in liver fibrosis," *Seminars in Liver Disease*, vol. 37, no. 2, pp. 119–127, 2017.

[44] X. K. Zhao, L. Yu, and M. L. Cheng, "Focal adhesion kinase regulates hepatic stellate cell activation and liver fibrosis," *Scientific Reports*, vol. 7, no. 1, pp. 4032–4063, 2017.

[45] Z. Dong, L. Su, S. Esmaili et al., "Adiponectin attenuates liver fibrosis by inducing nitric oxide production of hepatic stellate cells," *Journal of Molecular Medicine*, vol. 93, no. 12, pp. 1327–1339, 2015.

[46] L. Chen, R. Chen, S. Kemper, M. Cong, H. You, and D. R. Brigstock, "Therapeutic effects of serum extracellular vesicles in liver fibrosis," *Journal of Extracellular Vesicles*, vol. 7, no. 1, pp. 1461–1505, 2018.

[47] J. Qu, Z. Yu, Q. Li et al., "Blocking and reversing hepatic fibrosis in patients with chronic hepatitis B treated by traditional Chinese medicine (tablets of biejia ruangan or RGT): study protocol for a randomized controlled trial," *Trials*, vol. 15, no. 1, pp. 438–445, 2014.

[48] J. Lee, J. Yang, J. Jeon, H. Sang Jeong, J. Lee, and J. Sung, "Hepatoprotective effect of aesculetin on ethanol-induced liver injury in human HepG2 cells and C57BL/6J mice," *Journal of Functional Foods*, vol. 40, no. 18, pp. 536–543, 2018.

[49] A. Pandey, P. Raj, S. K. Goru et al., "Aesculetin ameliorates hepatic fibrosis in high fat diet induced non-alcoholic fatty liver disease by regulation of FoxO1 mediated pathway," *Pharmacological Reports*, vol. 69, no. 4, pp. 666–672, 2017.

[50] F. Wang, J.-C. Liu, R.-J. Zhou et al., "Apigenin protects against alcohol-induced liver injury in mice by regulating hepatic CYP2E1-mediated oxidative stress and PPARα-mediated lipogenic gene expression," *Chemico-Biological Interactions*, vol. 275, no. 14, pp. 171–177, 2017.

[51] Y. Lv, X. Gao, Y. Luo et al., "Apigenin ameliorates HFD-induced NAFLD through regulation of the XO/NLRP3 pathways," *The Journal of Nutritional Biochemistry*, vol. 71, no. 8, pp. 110–121, 2019.

[52] H. Qiu, J. Ma, H. Wu, and C. Ding, "DL-3-n-butylphthalide improves ventricular function, and prevents ventricular remodeling and arrhythmias in post-MI rats," *Naunyn-Schmiedeberg's Archives of Pharmacology*, vol. 391, no. 6, pp. 627–637, 2018.